Transferability of the Valence Ionization Intensities of Chemical Functional Groups between Molecules†

Julia K. Padden Metzker, Nadine E. Gruhn, and Dennis L. Lichtenberger*

Center for Gas-Phase Electron Spectroscopy, Department of Chemistry, The University of Arizona, Tucson, Arizona 85721

Received: March 18, 2002; In Final Form: August 7, 2002

The transferability of the valence ionization intensities of chemical functional groups is investigated with three common laboratory ionization sources (Ne Iα, 16.7 eV; He Iα, 21.2 eV; and He IIα, 40.8 eV) for a series of molecules. Each molecule contains two different functional groups that are well separated electronically and spatially by an alkane chain linker. The optimum length of the alkane chain between the functional groups is investigated. In this initial study, the functional groups are RCl, RBr, RSH, and RFc, where R is an alkane chain and Fc is ferrocene with an alkane chain bonded to one cyclopentadienyl ring. An additional feature of this study is that each functional group contains a molecular orbital with nearly pure atomic character, allowing comparison to theoretical atomic ionization cross-section ratios. In general, the observed photoelectron intensity changes are more gradual than those predicted by either theoretical atomic photoionization cross sections or by a complete Gelius analysis based on molecular orbital compositions obtained from electronic structure calculations. Experimentally, there is a high degree of transferability of the relative ionization intensities of the chemical functional groups between the molecules of this set. These results indicate that an empirical library of the relative ionization cross sections of chemical functional groups as a function of photon energy will be a useful aid to the study of more complex molecules and will provide an experimental foundation for further theoretical studies of molecular photoelectron cross sections.

Introduction

Photoionization is one of the most basic processes resulting from the interaction of electromagnetic radiation with atoms and molecules.[1] The probabilities of photoionization in terms of photoionization cross sections are of fundamental importance to understanding many processes related to atomic and molecular spectroscopy[2−4] and also are utilized in numerous other areas of science and technology,[5,6] including atmospheric and space sciences,[7] radiation biophysics,[8] and biomedical radiolysis.[9]

Our particular interest in understanding photoionization cross sections arises from their value in revealing electronic structure and bonding information from the photoelectron spectra of inorganic and organometallic molecules.[10−14] Some of the most useful information for assigning and interpreting ionizations of molecules has come from the comparison of spectra obtained with different photon energies, because the photoionization cross section is dependent upon the energy of the ionizing photon and the character of the molecular orbital. This information has been used since the earliest days of molecular photoelectron spectroscopy,[15,16] and variable energy photon studies have become increasingly common since the advent of high-intensity tunable synchrotron radiation sources.[12,17] The general trends that have been observed for photoionization behavior often lead to a clear and convenient differentiation between ionizations from metal-based and ligand-based orbitals in the photoelectron spectra of inorganic and organometallic molecules.

The computation of theoretical photoionization cross sections also has advanced considerably in recent years and continues to be an important area of activity.[18−29] Similar to the experimental studies, the computed partial cross sections of molecular ionizations are often compared to the sums of cross sections of the constituent atomic ionizations.[23,25] In many cases the atomic model gives reasonable account of the general trends in cross-section behavior, but the differences also point to important aspects of molecular behavior beyond the atomic model. We and others have found significant deviations from expected trends, particularly for molecules with highly delocalized orbitals,[30,31] molecules that have ionizations with different vibrational or vibronic contributions to the intensity,[12,32] and molecules with channels of excitations that compete with direct ionization (i.e., autoionization, photodissociation, charge-transfer satellites, etc.).[31,33] These problems often manifest themselves in studies of valence ionizations with low photon energies close to threshold.[34] In addition to possible molecular effects and questions of the assumptions used in the calculations of theoretical values for molecules, factors associated with instrumental design are also important to the observed valence ionization intensity due to the additional dependence of intensity on the angle between the ionization source vector and the path of the analyzed electrons, as defined by the asymmetry parameter, which is also dependent on vibrational and other molecular effects.[35,36]

Our purpose in this work is to examine molecular valence ionization intensity in terms of chemical functional groups in molecules rather than atoms in molecules. The first question concerns the extent to which the atomic and molecular factors that determine the partial photoionization cross section of a functional group ionization transfer from molecule to molecule. Do the intensity behaviors of functional group ionizations provide a more effective approach to assigning molecular

† Part of the special issue "Jack Beauchamp Festschrift".

* To whom correspondence should be addressed. E-mail: dlichten@u.arizona.edu.

10.1021/jp025783k CCC: $22.00
Published on Web 08/30/2002

ionizations than present approaches based on atomic cross sections, and can deviations from transferability reveal features of molecular electronic structure and behavior? For this initial study, we have chosen a relatively simple series of molecules and commonly used laboratory ultraviolet ionization sources to test the ability to transfer relative ionization cross sections of functional groups from molecule to molecule. The functional groups that have been selected for this study have valence ionizations from highly localized orbitals and therefore can also test the value of the sum of calculated relative cross sections of the constituent atoms for prediction of relative cross sections for ionization of molecules. The measure of relative ionization cross sections of functional groups in molecules can provide a foundation for more advanced theoretical calculations of molecular cross section behavior and can also provide an empirical basis for future interpretations of the ionization intensity behavior of other molecules.

Experimental Section

Sample Preparation. 1-Chloropropane, 1-propanethiol, and 3-chloro-1-propanethiol were used as obtained from Aldrich. The bromochloroalkanes were purchased from Fluka and used without modification. 6-Ferrocenylhexanethiol and 6-bromohexylferrocene were prepared according to published procedures[37] modified to obtain appropriate alkane chain lengths.

Photoelectron Spectra. All of the samples with the exception of the ferrocene derivatives are liquids and were introduced to the spectrometer from a sealed glass tube with a sidearm attached to an internal stainless steel tube via a variable leak valve. No heating was necessary for vaporization of these liquid samples. Spectra for the ferrocene derivatives were measured from an aluminum sample cell at 90−100 °C. The instrument and sample cell designs have been described in detail previously.[38,39] It is important to note that the angle between the incident photon flux and the outgoing electron path in our experimental design is centered at 90°. The ionization source photons used in this work are generated from the Ne Iα (16.7 eV), He Iα (21.2 eV), and He IIα (40.8 eV) resonance lines. Spectra are corrected for ionizations due to He Iβ and He IIβ excitations, for the spin−orbit splitting of the Ne Iα line, and also for the instrumental sensitivity as a function of electron kinetic energy.

Relative Ionization Intensities. The ionization bands are represented analytically with asymmetric Gaussian peaks defined by peak position, high and low half-widths, amplitude, and a linear baseline.[40,41] The peak areas, used for relative cross section analyses, are determined using Simpson's rule for integration of parabolic peaks.[42] In the case of overlapping peaks, the overlapping half-widths in a given spectrum might not be independently determined, and in these cases, the peak half-widths are constrained to values obtained from related spectra that do not have the overlap problem to maintain consistent comparisons of peak areas between the spectra. Once peak areas are obtained, they are normalized to the number of electrons in the ionized orbital to provide one-to-one electron cross-section ratios that can be compared directly to the calculated atomic cross-section ratios in the tables, which are similarly normalized in this work to the number of electrons in the shells. The error in the area for well-separated ionization peaks, as is the case for 3-chloro-1-propanethiol, is typically less than 2%.[43] Peak areas for highly overlapping peaks with reasonable intensity such as the sulfur lone-pair ionization in the Ne I and He I photoelectron spectra of 6-ferrocenylhexanethiol possess an uncertainty in the 5−10% range. Low-intensity ionizations such as the sulfur lone-pair ionizations in the He II spectra can result in uncertainties for peak areas in the 10−20% range depending on the overlap with other ionizations, the availability of good half-widths from other spectra, and the certainty of the baseline.

Calculations. Density functional molecular orbital calculations were performed using the Amsterdam density functional (ADF) program, version 2000.01,[44−47] to assess the atomic character in the functional groups of interest. The local density approximation to the exchange potential and gradient corrections to exchange (Becke)[48] and correlation (LYP)[49] were implemented in all cases with a frozen-core triple-ξ basis set on all atoms except hydrogen where a double-ξ basis set was employed. Density functional calculations were also performed using the B3LYP hybrid functional and the LANL2DZ basis set in Gaussian 98[50] for comparison. The orbital compositions from Gaussian 98 are very similar to those obtained with ADF, and only the ADF results are presented here. For longer alkane chains ($n \geq 4$), the lowest-energy conformers were determined from a systematic search and molecular mechanics comparison of conformers performed with Spartan[51] using the AM1 force field for simple organic molecules and the MMFF94X force field for ferrocene derivatives. Selected conformers were subsequently geometry-optimized in ADF. In all cases, the lowest-energy conformer adopted an all trans conformation, thus keeping the functional groups well-separated in space.

Preliminary Considerations

Measurements of absolute cross sections by gas-phase photoelectron spectroscopy are dependent on photon flux, sample flux, and instrument geometries and largely have been carried out only for inert gases and small molecules.[7,52−54] However, a useful database for assigning and interpreting molecular ionizations only requires the relative intensities of functional group ionizations for a given instrument design. With the goal of obtaining relative ionization intensities for functional groups, we set about collecting ultraviolet photoelectron spectra for a series of molecules containing two functional groups separated by a linker unit as depicted below. The ratio of the integrated intensity of a valence ionization associated with functional group A to the integrated intensity of a valence ionization associated with functional group B in a molecule k is designated $[I(\mathrm{A})/I(\mathrm{B})]_k$.

The design and analysis of this model system is critical for obtaining useful ionization intensity ratios. In this study, we use an alkane chain as a linking unit to connect the functional groups to one another. The advantage of this system is that through judicious choice of functional group electronegativities and the number of CH_2 groups in the alkane chain the degree of orbital mixing between functional groups is easily controlled. Longer length chains allow for greater separation of the functional groups, but as will be shown, it is helpful to keep the length of the chain relatively short ($n \leq 6$) to prevent two important drawbacks: interference of the alkane chain ionization peaks with the ionization peaks of interest and formation of conformers that can lower the symmetry and increase the possibility of orbital mixing between functional groups. The interaction between the alkane chain and the functional groups is assessed in the course of this study.

The measured relative ionization intensities reflect the relative partial photoionization cross sections for the valence ionizations at the angle of electron collection. To aid with comparison to

TABLE 1: Theoretical Relative Atomic Partial Ionization Cross Sections[a]

atomic orbital	Ne I (16.7 eV)	He I (21.2 eV)	He II (40.8 eV)
H 1s	1.929	1	0.154
C 2p	2.197	1.624	0.499
S 3p	2.422	0.58	0.08
Cl 3p	5.041	1.473	0.068
Br 4p	4.101	1.653	0.102
Fe 3d	0.316	0.428	0.774

[a] Values calculated from Yeh's theoretical atomic subshell cross-section values[55] normalized to the H 1s cross section with He I excitation and normalized by the number of electrons in the atomic subshell. The theoretical absolute cross section for H 1s ionization is 1.884 Mb.

calculated ratios of atomic ionization cross sections, we have chosen as our starting point functional groups with one or more molecular orbitals with a high degree of localization in a single atomic orbital. Later studies may involve extension to functional groups containing several atoms (olefins, carbonyls, amides, etc.). The functional groups that we have chosen for this study are RBr, RCl, RSH, and RFc where R is an alkane chain and Fc is ferrocene with the alkane chain substituted for a hydrogen on one cyclopentadienyl ring. The valence ionizations of interest are the "lone-pair" ionizations of the main group atoms, labeled Br_{lp}, Cl_{lp}, and S_{lp}, and the Fe 3d-based $^2A_{1g}$ and $^2E_{2g}$ ionizations of ferrocene, labeled collectively Fc_{3d}. Ionization intensity ratios are determined from relative photoelectron peak areas in the photoelectron spectra of molecules with pairs of these atoms/groups connected by alkane chains. We report experimentally determined intensity ratios for bromine relative to chlorine lone-pair ionizations (Br_{lp}/Cl_{lp}), chlorine relative to sulfur lone-pair ionizations (Cl_{lp}/S_{lp}), sulfur lone-pair relative to metallocene iron 3d ionizations (S_{lp}/Fc_{3d}), and bromine lone-pair relative to metallocene iron 3d ionizations (Br_{lp}/Fc_{3d}).

There are several tabulations of calculated theoretical photoionization cross sections of atoms available for comparison.[55−58] Yeh and Lindau[55,56] have calculated theoretical one-electron cross sections for nearly all atomic subshells using the Hartree−Fock−Slater dipole approximation and specifically listed values for the common laboratory photon sources. These values are often used for interpretations of valence molecular photoionization intensities.[59−63] Yeh's values agree well with the more recent results of Verner et al.[57] for the sulfur, chlorine, and iron valence ionizations, but the latter work does not extend to the bromine atom. The agreement of these calculated values with measurements of absolute photoionization cross sections is very good for light atoms in absence of other effects and less good for the heavier elements, although general trends are preserved. For molecules, the simple model of Gelius[64,64] is often employed, especially for transition metal systems.[12,17,61] In this model, the cross-section behavior of molecular ionizations is assumed to be dependent only on the sum of the atomic ionization cross sections weighted according to the atomic orbital contributions to the molecular orbitals. This model is most applicable for ionization by high-energy (X-ray) photons and is less appropriate for near-threshold ultraviolet photons typically used to evaluate valence ionizations of molecules, for which the understanding of orbital character is most important. The appropriateness of this model will be examined for the well-defined molecular systems reported here.

The atomic cross sections calculated by Yeh[55,56] for the elements relevant to this present work are listed in Table 1. Generally, as the ionization source energy is increased above the threshold energy, the cross sections for halogen orbital ionizations decrease dramatically, cross sections for C 2p orbital ionizations decrease slightly, and cross sections for iron 3d orbital ionizations increase modestly. These trends compare in at least a general way with the relative intensity trends often observed for ionizations of inorganic and organometallic molecules. As a result of these traits, the cross sections for ionizations from molecular orbitals that are predominantly ligand in character typically decrease with increasing source energy relative to those from primarily metal-based orbitals.

TABLE 2: Theoretical One-Electron Atomic Partial Ionization Cross-Section Ratios[a]

	Ne I (16.7 eV)	He I (21.2 eV)	He II (40.8 eV)
Br_{4p}/Cl_{3p}	0.816	1.122	1.500
Cl_{3p}/S_{3p}	2.081	2.540	0.850
S_{3p}/Fe_{3d}	7.655	1.355	0.103
Br_{4p}/Fe_{3d}	12.978	3.862	0.132

[a] Ratios determined using the theoretical one-electron atomic cross-sections in Table 1.

The series of molecules studied here provides a circular internal check of the transferability of functional group ionization intensities between molecules in that the product of three intensity ratios will provide a test of the fourth intensity ratio, as depicted below in eq 1, where the individual ratios are

$$\left[\frac{I(\mathrm{Br_{lp}})}{I(\mathrm{Cl_{lp}})}\right]_a \times \left[\frac{I(\mathrm{Cl_{lp}})}{I(\mathrm{S_{lp}})}\right]_b \times \left[\frac{I(\mathrm{S_{lp}})}{I(\mathrm{Fc_{3d}})}\right]_c \approx \left[\frac{I(\mathrm{Br_{lp}})}{I(\mathrm{Fc_{3d}})}\right]_d \quad (1)$$

measured for molecules a, b, c, and d. This internal consistency is illustrated if the relative ionization intensities in eq 1 are replaced by the purely atomic photoionization cross sections as in eq 2. The atomic cross-section ratios from eq 2 calculated

$$\frac{\sigma(\mathrm{Br_{4p}})}{\sigma(\mathrm{Cl_{3p}})} \times \frac{\sigma(\mathrm{Cl_{3p}})}{\sigma(\mathrm{S_{3p}})} \times \frac{\sigma(\mathrm{S_{3p}})}{\sigma(\mathrm{Fe_{3d}})} = \frac{\sigma(\mathrm{Br_{4p}})}{\sigma(\mathrm{Fe_{3d}})} \quad (2)$$

using Yeh's theoretical atomic cross-section values are given in Table 2. Of course, in this case, the equation is an exact equality. The product of three of the ratios is exactly the fourth for the isolated atomic values. A similar table using eq 1 will be constructed using the experimentally measured relative molecular ionization intensities presented in the next section. Each ratio in eq 1 is measured for a different molecule, and the extent that the relationship in eq 1 is true is an indication of the extent that the cross-section ratios are transferable between molecules.

When comparing the experimental molecular ionization intensities reported in this study to theoretical ionization cross sections, it is important to note that in our instrument the angle between the ionizing photon source and the photoelectron propagation vector is centered at 90°. The complete differential photoionization cross section ($d\sigma_{nl}/d\Omega$) for a randomly oriented sample in an unpolarized field at this geometry of 90° is given by eq 3[65] where β, known as the asymmetry parameter,

$$\frac{d\sigma_{nl}}{d\Omega} = \frac{\sigma_{nl}}{4\pi}\left[1 + \frac{1}{4}\beta(h\nu)\right] \quad (3)$$

determines the angular distribution displayed by ionized photoelectrons. The asymmetry parameter for ionization is dependent on the nature of the orbital, as well as the energy of the ionizing photon, and therefore does not cancel out in the cross-section ratio. Yeh and Lindau have calculated asymmetry parameters for atomic orbital ionizations over a wide range of photon energies, and those relevant to the present study are listed in

TABLE 3: Theoretical Atomic Asymmetry Parameters (β)[a]

atomic orbital	Ne I (16.7 eV)	He I (21.2 eV)	He II (40.8 eV)
H 1s	2	2	2
C 2p	1.162	1.309	1.505
S 3p	1.696	1.85	0.123
Cl 3p	1.39	1.774	−0.194
Br 4p	1.521	1.783	1.377
Fe 3d	0.211	−0.16	0.181

[a] Values from Yeh's theoretical atomic subshell cross-section calculations.[55]

Table 3. The extent to which these asymmetry parameters for atomic orbital ionizations might transfer to asymmetry parameters for molecular ionizations is not clear. The asymmetry parameter is also subject to molecular effects related to vibrational states, vibronic coupling, and other effects mentioned previously. The question again arises as to the extent that these molecular effects influence the transferability of relative functional group ionization intensities from molecule to molecule. For comparison to atomic models, theoretical atomic asymmetry parameters will be used to qualitatively assess the potential dependence of the cross-section ratios on variations in the asymmetry parameter, but more exact treatment of this effect requires a more detailed study.

Photoelectron Spectra

The variable photon energy (Ne Iα, 16.7 eV; He Iα, 21.2 eV; and He IIα, 40.8 eV) photoelectron spectra for the four molecules used to determine experimental ratios for eq 1 are presented in this section. General experimental observations are summarized here, and more detailed comparisons between the experimental molecular and theoretical atomic cross-section ratios are addressed in the Discussion. The He I photoelectron spectra for 1-chloropropane, 1-propanethiol, and 3-chloro-1-propanethiol presented in Figure 1 illustrate the approach used in this study. The photoelectron spectrum of 1-chloropropane is dominated by the sharp chlorine lone-pair ionizations (predominantly the two Cl 3p orbitals that are π with respect to the C−Cl bond) at 10.86 eV followed by ionizations of electrons from the Cl−C, C−C, and C−H σ bonds at higher ionization energy. The sharp peak at 9.19 eV in the photoelectron spectrum of 1-propanethiol is attributed to ionizations from the sulfur lone pair (predominantly the S 3p orbital perpendicular to the C−S−H plane), and the broad ionization envelope between 10.5 and 15 eV is due to electrons ionized from the σ-bond framework. The lowest-energy feature in the region of σ-bond ionizations for 1-propanethiol is the S−C σ-bond (predominantly S 3p in character) ionization located at 11.3 eV. The second sulfur lone-pair orbital that is predominantly S 3s in character is at much lower energy than the predominantly S 3p lone pair and is obscured by the ionizations from the σ-bond framework.[66]

The prominent features in the photoelectron spectra of 1-chloropropane and 1-propanethiol are also present in the spectrum of 3-chloro-1-propanethiol, which is essentially the sum of the two previous spectra. The chlorine lone-pair and the sulfur lone-pair ionization peaks retain their sharp profiles, and both are only slightly stabilized in energy indicating little interaction between functional groups. The chlorine lone-pair ionization energy has been stabilized by 0.16 eV, and the sulfur lone pair from the thiol group has been stabilized by 0.21 eV. The sulfur lone-pair ionization is stabilized to a greater degree than the chlorine lone-pair ionization because of the higher electronegativity of chlorine. Additionally, ionizations from the

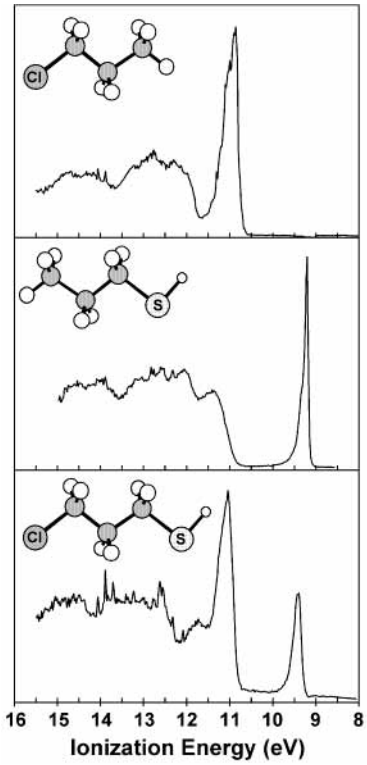

Figure 1. Valence He I photoelectron spectra of 1-chloropropane, 1-propanethiol, and 3-chloro-1-propanethiol.

σ-bond framework in 1-propanethiol have been stabilized, and in particular, the ionization of 1-propanethiol at 11.3 eV has been stabilized to 11.7 eV and therefore does not obscure the chlorine lone-pair ionization in the 3-chloro-1-propanethiol spectrum. The Cl and S 3p lone-pair ionizations are well-separated and baseline-resolved from each other ensuring a high certainty in the measurement of their relative peak areas and determination of their relative partial photoionization cross sections.

Chain-Length Dependence. A series of bromochloroalkanes, $Br(CH_2)_nCl$, with different alkane chain lengths $n = 1$, 3, 4, and 6 was examined to assess the effect of changing the length of the alkane chain separating the two functional groups. The He I photoelectron spectra for this series are presented in Figure 2. In each of these spectra, the single intense peak at 11−12 eV is assigned to the chlorine lone-pair ionizations. The doublet at 10−11 eV is the spin−orbit split bromine lone-pair ionizations. The spin−orbit splitting of the bromine lone-pair ionizations remains constant (0.28−0.30 eV) throughout the series. This observation and the observation that the chlorine lone-pair ionizations remain degenerate within the resolution of the experiment indicate that the mixing between the chlorine and bromine lone pairs is not substantial. As CH_2 groups are added, intensity emerges in the 11.5−15 eV range because of the additional C−C and C−H σ-bond ionizations. It can be seen from the spectrum of the $n = 6$ case that the C−C and C−H σ-ionization profile is beginning to overlap with the ionization peaks of interest.

Br_{lp}/Cl_{lp}. The variable photon energy photoelectron spectra for the key ionizations of 1-bromo-4-chlorobutane are shown in Figure 3. These spectra are fit with Gaussian peaks to determine the peak areas analytically. In this and each of the following spectral figures, the actual data points are shown as vertical lines (the length of each data point line represents the experimental variance)[41] and the sum of the Gaussians used to represent the data is shown as a solid line to indicate the

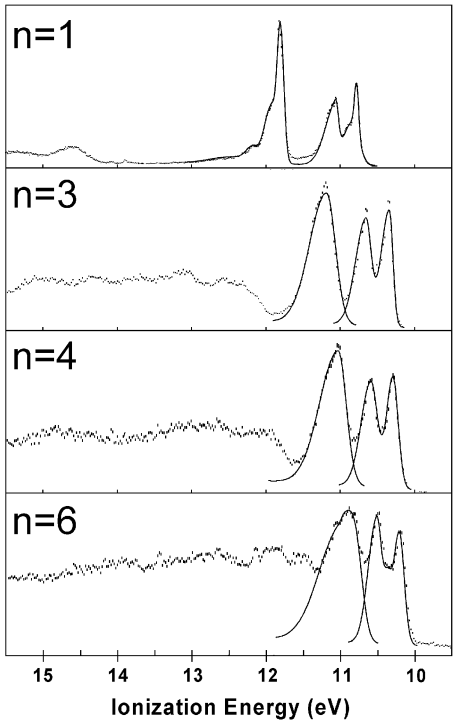

Figure 2. Valence He I photoelectron spectra of bromochloroalkanes, $Br(CH_2)_nCl$, where $n = 1$, 3, 4, and 6.

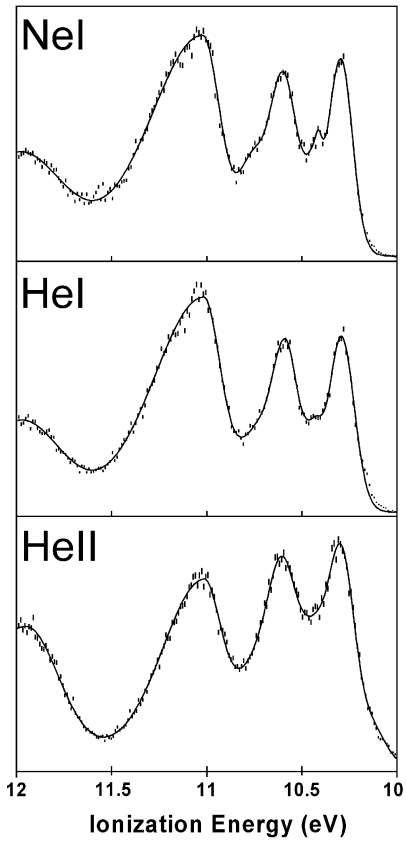

Figure 3. Photoelectron spectra of 1-bromo-4-chlorobutane collected with Ne I, He I, and He II ionization sources.

agreement between the data points and the analytical representation. The individual Gaussians used to obtain the fits are not meant to imply any chemical significance, such as the number or energy of individual positive ion states or the frequency of vibrational progressions, but are merely optimized to obtain the most accurate and consistent analytical representation of the area under each ionization band. The data for this and subsequent spectral figures are reproduced in the Supporting Information with the individual Gaussians shown, as well as additional analytical information reported in tabular form.

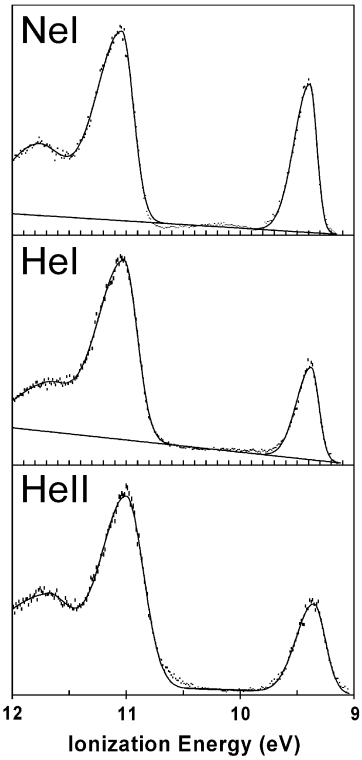

Figure 4. Photoelectron spectra of 3-chloro-1-propanethiol collected with Ne I, He I, and He II ionization sources.

The theoretical atomic cross sections in Table 1 predict a steady increase in bromine 4p ionization intensity relative to chlorine 3p intensity as photon energy is increased. It is visually apparent from comparison of the He I and He II spectra in Figure 3 that there is an increase in the bromine lone-pair ionization intensity relative to the chlorine lone-pair ionization intensity. The chlorine and bromine lone-pair intensities show little relative change, however, between the Ne I and He I spectra.

Cl_{lp}/S_{lp}. Figure 4 shows the photoelectron spectra of 3-chloro-1-propanethiol with different photon sources. As the photon energy is increased from Ne I to He I, the chlorine lone-pair ionizations demonstrate a significant increase in intensity with respect to the sulfur lone-pair ionization analogous to the trend predicted by the theoretical photoionization cross-section values for chlorine 3p and sulfur 3p atomic orbitals. On the other hand, the relative chlorine and sulfur lone-pair ionization peak intensities show little change between the He I and He II spectra despite the significant decrease in chlorine atomic photoionization cross section relative to sulfur predicted from the atomic values in Table 1.

Br_{lp}/Fc_{3d}. Figure 5 shows the photoelectron spectra of 6-bromohexylferrocene with different photon sources. Apart from the two sharp ionizations at 10.05 and 10.36 eV, which correspond to the spin−orbit split bromine lone-pair ionizations, the spectra are similar to the photoelectron spectra of unsubstituted ferrocene.[14,67−69] The bromine spin−orbit splitting value of 0.31 eV observed for this molecule is comparable to that of the bromochloroalkane series. The ionization envelope from 6.5 to 7.5 eV consists of ionizations from the metallocene iron 3d-based orbitals. The broad ionization peak at 6.74 eV originates from a doubly degenerate molecular orbital that is predominantly iron d_{xy}, $d_{x^2-y^2}$ in character. The sharper ionization at 7.12 eV

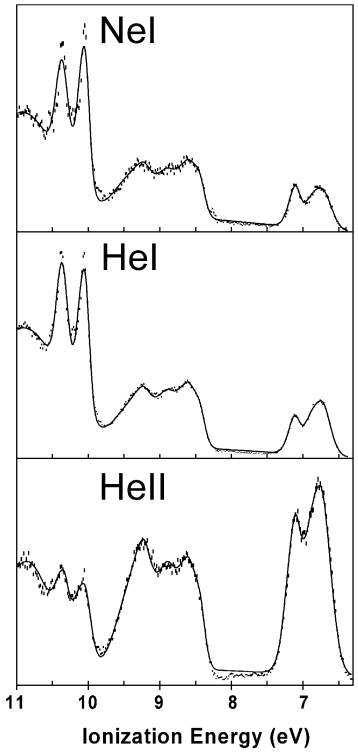

Figure 5. Photoelectron spectra of 6-bromohexylferrocene collected with Ne I, He I, and He II ionization sources.

originates from a molecular orbital that is almost entirely iron d_{z^2} in character.[14] To use notations for the D_{5d} point group, these two ionizations correspond to removal of electrons from the e_{2g} and a_{1g} symmetry orbitals. The area from 8 to 10 eV represents electrons ionized from Cp π-based molecular orbitals. Each section of the spectrum was fit with a separate linear baseline to account for the increased scattering at higher kinetic energies. Similar to the predicted trends for iron 3d and bromine 4p atomic orbitals, the metal-based ionizations demonstrate a striking increase in intensity relative to the bromine lone-pair ionizations as the photon energy is increased from He I to He II. Little change is observed from Ne I to He I excitation.

S_{lp}/Fc_{3d}. Figure 6 shows the photoelectron spectra of 6-ferrocenylhexanethiol with different photon sources. The spectrum has very similar features to the spectrum of 6-bromohexylferrocene (Figure 5) in the region below 7.5 eV, corresponding to the ferrocene-based e_{2g} and a_{1g} ionizations. The Cp π-based ionization envelope from 8 to 9.5 eV and the sulfur lone-pair ionization at 9.21 eV overlap extensively. The high degree of overlap between these ionizations requires special care in obtaining an analytical fit of this region for comparison of the relative cross sections. The Cp π-ionization profile for this molecule was fit using the ionization profile shape from the Cp π-ionization peaks in the 6-bromohexylferrocene spectra. Any extra intensity in this range is attributed to the sulfur lone-pair ionization. Regardless of the method for obtaining the analytical fits, it is visually clear that as the ionization source energy is increased the sulfur-based ionization peak dramatically falls off in intensity when compared to the metal-based $^2E_{2g}$ and $^2A_{1g}$ ionization peaks.

Discussion

Transferability. Table 4 collects the experimentally determined valence ionization intensity ratios for the functional groups in the molecules of this study. The ratios are normalized to the area per electron to facilitate comparison of experimental

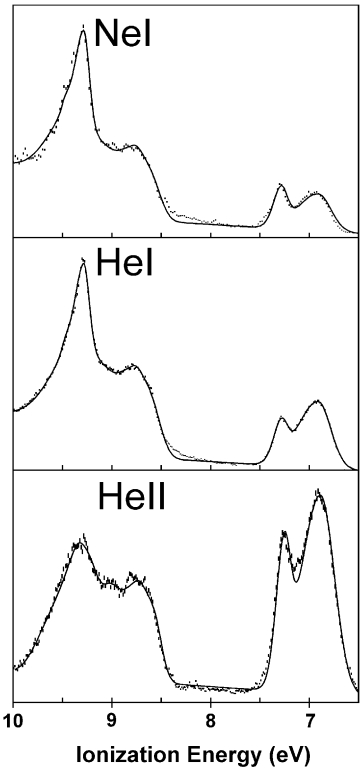

Figure 6. Photoelectron spectra of 6-ferrocenylhexanethiol collected with Ne I, He I, and He II ionization sources.

TABLE 4: Experimental Molecular Ionization Intensity Ratios of Functional Groups[a]

	Ne I (16.7 eV)	He I (21.2 eV)	He II (40.8 eV)
Br_{lp}/Cl_{lp}	0.89	0.85	1.66
Cl_{lp}/S_{lp}	1.07	1.75	1.59
S_{lp}/Fc_{3d}	4.36	2.15	0.21
Br_{lp}/Fc_{3d}	3.76	3.43	0.53
predicted Br_{lp}/Fc_{3d}	4.15	3.20	0.55
% difference	+9%	−7%	+4%

[a] Ratios obtained from gas-phase photoelectron spectra of $Br(CH_2)_4Cl$, $Cl(CH_2)_3SH$, $Fc(CH_2)_6SH$, and $Fc(CH_2)_6Br$ normalized by the number of electrons of the indicated types. The labels refer to the primary molecular orbital characters associated with the ionizations. The halogen lone-pair ratios combine the in-plane and out-of-plane lone-pair ionizations. The Fc_{3d} label combines the ferrocene-based $^2A_{1g}$ and $^2E_{2g}$ ionizations.

molecular ionization intensity ratios with theoretical atomic cross-section ratios. As mentioned previously, the circular series of functional groups chosen provides an estimate of the internal consistency and transferability of the functional group ionization intensities. Specifically, the product of the first three ratios, Br_{lp}/Cl_{lp}, Cl_{lp}/S_{lp}, and S_{lp}/Fc_{3d}, should closely predict the ratio measured for Br_{lp}/Fc_{3d}. The difference between the predicted Br_{lp}/Fc_{3d} ratio and the actual value is a measure of the transferability among this group of molecules. The transferability is very good in comparison to the certainty in the determination of the relative ionization peak areas. This is particularly true for the set of ionizations measured with the He II source, for which there was considerable uncertainty in the determination of the very low intensity of the sulfur and bromine lone-pair ionizations that overlap with the substituted ferrocene ionizations. The agreement of the measured and predicted Br_{lp}/Fc_{3d} ionization intensity ratio within 4% suggests some cancellation of errors. No particular significance is placed on the improvement in transferability as the energy of the photon source is

TABLE 5: Molecular Orbital Atomic Character as Predicted by ADF Density Functional Calculations[a]

	C−C σ	C−S σ	Cl (∥)	Cl (⊥)	S lp
		$Cl(CH_2)_3SH$			
eigenvalues	−8.84	−8.16	−6.96	−6.94	−5.60
S	1%	61%			93%
Cl	2%		88%	89%	
C	48%	21%	6%	4%	2%
H	46%	13%	2%	6%	4%
		$Br(CH_2)Cl$			
	C−C σ	Cl (∥)	Cl (⊥)	Br (∥)	Br (⊥)
eigenvalues	−10.44	−7.62	−7.54	−6.95	−6.88
Br	44%	21%	9%	84%	87%
Cl	17%	73%	86%	14%	5%
C	35%				2%
H	2%	2%	3%		4%
		$Br(CH_2)_4Cl$			
	C−C σ	Cl (∥)	Cl (⊥)	Br (∥)	Br (⊥)
eigenvalues	−8.60	−7.01	−6.97	−6.55	−6.53
Br	27%	5%		90%	94%
Cl	10%	85%	89%	3%	
C	44%	5%	4%	3%	2%
H	11%		6%		3%
		$Br(CH_2)_6Cl$			
	C−C σ	Cl (∥)	Cl (⊥)	Br (∥)	Br (⊥)
eigenvalues	−8.24	−6.86	−6.85	−6.44	−6.42
Br	22%	1%		91%	94%
Cl	8%	86%	89%	3%	
C	53%	5%	2%		1%
H	2%		6%		3%
		$Fc(CH_2)_6SH$			
	C−C σ	S lp	Fe (a_{1g})	Fe (e_{2g})	Fe (e_{2g})
eigenvalues	−5.60	−5.35	−4.20	−3.82	−3.80
Fe			93%	82%	82%
S	5%	92%			
C	82%	2%		13%	9%
H	2%	2%			
		$Fc(CH_2)_6Br$			
	Br (∥)	Br (⊥)	Fe (a_{1g})	Fe (e_{2g})	Fe (e_{2g})
eigenvalues	−6.34	−6.28	−4.17	−3.77	−3.69
Br	93%	92%			
Fe			93%	82%	83%
C	2%			8%	5%
H		3%			

[a] The orbital labels follow from the primary character. The ∥ symbol indicates the in-plane lone-pair combination and the ⊥ symbol indicates the out-of-plane lone-pair combination with respect to the C−C−X plane.

increased, because all fall near the uncertainty in the experimental determination of the intensity ratios.

A point in the preliminary considerations for this study was to choose functional groups that contain orbitals that are largely atomic in nature. A more complete assessment of the orbital character of the Cl, Br, and S lone-pair molecular orbitals and the ferrocene a_{1g} and e_{2g} molecular orbitals is important for understanding the extent to which the experimental molecular ionization intensities are expected to transfer from molecule to molecule. The characters of these orbitals as obtained from density functional electronic structure calculations are collected in Table 5. The calculated orbital characters for 3-chloro-1-propanethiol show that the sulfur lone-pair orbital is 93% sulfur in character and the in-plane (∥) and out-of-plane (⊥) chlorine lone-pair orbitals are 88% and 89% chlorine in character. The remaining character in each case is primarily from the hydrocarbon chain. These values indicate that the chlorine and sulfur lone-pair ionizations are mostly atomic in character with essentially no interaction between the functional groups and with small orbital mixing between the functional groups and the alkane chain. Similar results are found for the other molecules in this study. The least-localized orbitals are the e_{2g} orbitals of ferrocene, which are 82% Fe in character. The delocalization of these orbitals is primarily to the cyclopentadienyl rings and remains essentially the same for both 6-ferrocenylhexanethiol and 6-bromohexylferrocene, so the orbitals retain their functional group character when considering the transferability of the ionization intensities.

TABLE 6: Theoretical Molecular Ionization Intensity Ratios from Full Gelius Analysis[a]

	Ne I (16.7 eV)	He I (21.2 eV)	He II (40.8 eV)
Br_{lp}/Cl_{lp}	0.844	1.116	1.228
Cl_{lp}/S_{lp}	1.958	2.327	0.998
S_{lp}/Fc_{3d}	5.323	1.212	0.127
Br_{lp}/Fc_{3d}	10.451	3.557	0.148
predicted Br_{lp}/Fc_{3d}	8.793	3.148	0.155
% difference	−19%	−13%	+5%

[a] Using orbital characters in Table 5 and atomic cross sections in Table 1. See Table 4 for explanation of labels.

To evaluate the effect of orbital delocalizations on intensities, a first-order analysis by the model of Gelius was performed for all molecules in this study. The Gelius analysis of the cross section for a particular molecular orbital is given by eq 4 where

$$\sigma_{MO} = \sum_{AO} k_{MO,AO}\sigma_{AO} \qquad (4)$$

σ_{MO} is the one-electron cross section for the molecular orbital and $k_{MO,AO}$ describes the extent to which each atomic orbital contributes to the molecular orbital. The implication of angular effects will be discussed later. For this analysis, $k_{MO,AO}$ is taken to be equal to the atomic orbital character in the molecular orbital as given in Table 5. The theoretical predictions using the Gelius ratios are summarized in Table 6. As this table shows, perfect transferability of the ionization intensities of functional groups is not to be expected because of variations in orbital characters. The deviations in the predicted He I and He II intensity ratios are similar to those obtained experimentally and suggest that the slight changes in orbital characters account for the lack of perfect transferability. To turn this around, differences in expected intensity ratios for functional groups between molecules indicate the changes in orbital character. The Gelius analysis does not help in understanding the deviation from perfect transferability of the Ne I cross sections. The calculated deviation by the Gelius model is in the opposite direction of that observed. This suggests that molecular effects are more important for low kinetic energy electrons, as might be expected.

Chain Length. The bromochloroalkane series in Figure 2 demonstrates how, as the number of methylene groups in the linking chain is increased, the increasingly destabilized combinations of C−C-bonding orbitals cause the alkyl ionization envelope (11.5−15 eV) to spread to lower ionization energy. This spreading can, depending on the functional group electronegativities, eventually encroach upon the functional group ionizations, as is seen in the $n = 6$ case. This spectral crowding

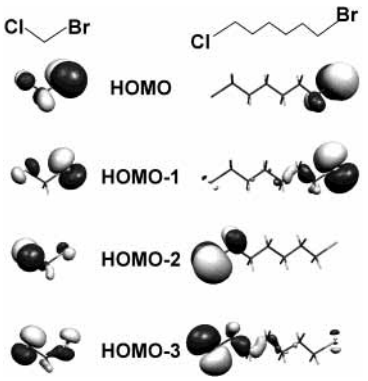

Figure 7. Contour plots of the primarily halide lone-pair orbitals of $Cl(CH_2)Br$ (left) and $Cl(CH_2)_6Br$ (right).

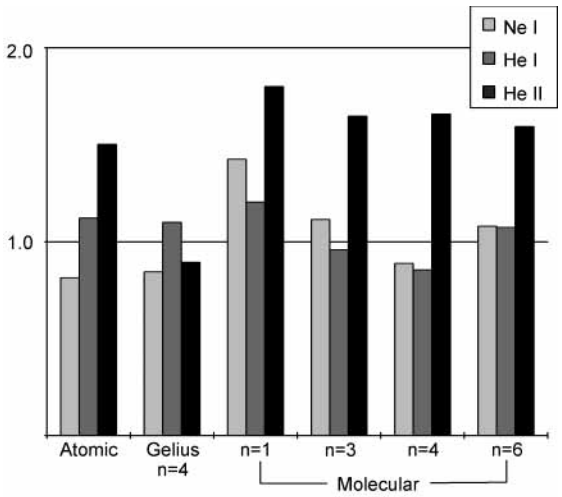

Figure 8. Theoretical atomic, Gelius, and functional group Br-to-Cl ionization intensity ratios for bromoalkanes, $Br(CH_2)_nCl$, where n = 1, 3, 4, and 6.

produces overlapping ionization peaks, reducing certainty in determining the individual peak areas and increasing error in the functional group partial cross-section ratios.

Bromine 3p and chlorine 2p orbitals have similar energies, and their functional group orbitals will therefore be prone to orbital mixing unless prevented by symmetry or spatial separation. 1-Bromo-1-chloromethane, with a Br−Cl calculated distance of 3.19 Å, has significant mixing between the chlorine and bromine in-plane (⎮⎮) lone-pair orbitals. The molecular orbital characters in Table 5 assign 14% of the predominantly bromine (⎮⎮) lone pair to atomic chlorine character and 21% of the predominantly chlorine (⎮⎮) lone pair to atomic bromine character. This degree of mixing can significantly alter intensity profiles for ionizations from these orbitals. The amount of orbital mixing between the chlorine and bromine lone pairs is reduced to less than 5% in the four and six carbon chain analogues. The reduction in mixing with increasing chain length is clearly depicted in the lone-pair molecular orbital pictures for 1-bromo-1-chloromethane and 6-bromo-1-chlorohexane shown in Figure 7. When the degree of orbital mixing and the separation of the ionization peaks for the Br and Cl functional groups is weighed, the $n = 4$ analogue is the optimum choice for intensity analysis and comparison to theoretical atomic cross-section ratios.

Figure 8 illustrates the bromine-to-chlorine lone-pair ionization intensity ratios for the entire bromochloroalkane series studied. The $n = 1-4$ analogues demonstrate parallel intensity trends in their Ne I, He I, and He II spectra. From $n = 1$ to $n = 4$, the ratios are approaching the ratios for "pure" isolated

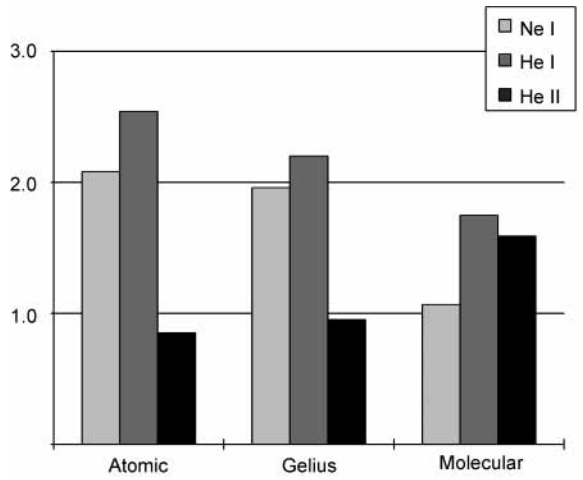

Figure 9. Theoretical atomic, Gelius, and functional group Cl-to-S ionization intensity ratios for 3-chloropropanethiol.

functional groups, but the ratios for $n = 6$ deviate from this convergence. The deviation for $n = 6$ from the three other molecules is likely a function of crowding in the spectra and the inherent difficulty of obtaining reliable ionization peak areas in a crowded spectrum.

Comparison to Atomic Cross-Section Trends. Because the functional groups contain molecular orbitals that are highly localized in individual atomic orbitals, it is instructive to compare the intensity ratios obtained experimentally for the functional group ionizations in these molecules with the cross-section ratios that have been calculated theoretically for the corresponding atomic ionizations, as described earlier. The experimental Br_{lp}/Cl_{lp} ratio values shown in Figure 8 do not exactly follow the stepwise increase in the Br_{4p}/Cl_{3p} ratio from Ne I to He I to He II excitation as predicted by the theoretical atomic cross-section ratios. Additionally, the experimental Br_{lp}/Cl_{lp} ratio values from He II spectra are somewhat larger than is predicted from the theoretical atomic and Gelius models.

It is noted that the theoretical atomic ratios depicted in Figure 8 do not include consideration of the asymmetry parameters. Asymmetry parameters for functional groups in these molecules are not known empirically, but atomic asymmetry parameters have been calculated for these atoms and their effect can be considered for purposes of illustration.[56] For example, the theoretical atomic asymmetry parameters for bromine and chlorine have little effect on the Br/Cl Ne I and He I cross-section ratios, but in He II, the atomic asymmetry parameters have the effect of increasing the bromine-to-chlorine ratio by about 30%, which becomes a much better prediction of the experimentally determined ratios. This suggests that in this case the theoretical atomic asymmetry parameter ratios approximately transfer from the atoms to the molecules. It should be stressed again that the validity of using theoretically determined asymmetry parameters for atoms to predict or explain molecular cross-section behavior is still of question. While both the bromine and chlorine functional groups are relatively "atomic-like" in the molecule (the functional group orbitals remain highly localized on the atom and do not significantly shift in energy), the asymmetry parameters and cross-section values calculated for atoms use a spherical atomic model, and atoms in molecules are not spherical.

The chlorine-to-sulfur functional group ionization intensity ratios illustrated in Figure 9 obtained from the photoelectron spectra for 1-chloro-3-propanethiol roughly reflect the trend predicted by the theoretical atomic cross-section values and the

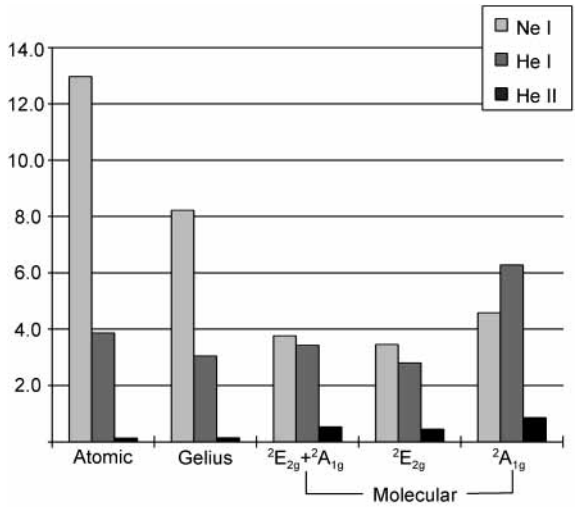

Figure 10. Theoretical atomic, Gelius, and functional group Br-to-Fe ionization intensity ratios for 6-bromohexylferrocene.

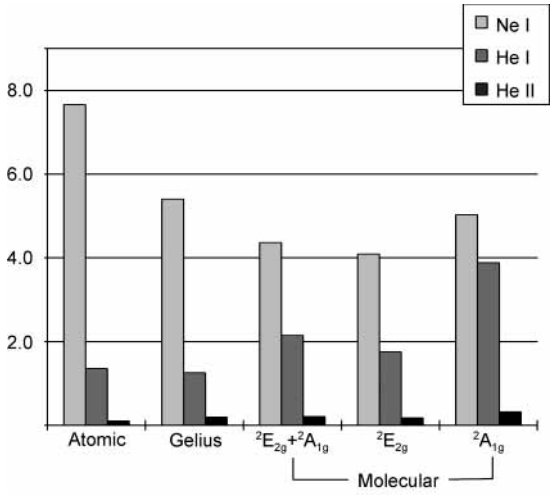

Figure 11. Theoretical atomic, Gelius, and functional group S-to-Fe ionization intensity ratios for 6-ferrocenylalkanethiol.

Gelius analysis, although the magnitude of the changes is smaller. The prevalent deviation occurs in the He II spectrum for which theory predicts a significant decrease in Cl 3p ionization intensity relative to S 3p when compared to those of He I. Instead, little change in the relative intensities is observed. The carbon character introduced into the functional group orbitals does not explain the reduction in the cross-section ratio changes. This effect is small, as can be seen from the Gelius cross-section ratios, which take into account orbital mixing within the molecule. Adjustment of the theoretical atomic and Gelius cross-section ratios for the atomic asymmetry parameters at our instrumental geometry leaves the theoretical chlorine-to-sulfur ratios essentially unchanged.

The theoretical atomic ratios predict a sharp decrease in bromine intensity relative to iron with increasing photon energy (Figure 10). The spectra demonstrate a small decrease in the bromine lone-pair ionization intensities relative to the iron-based e_{2g} and a_{1g} ionizations between Ne I and He I and a large decrease between He I and He II. Inclusion of the atomic asymmetry parameters has little influence on these trends. The difference between the theoretical and experimental ratios for this molecule is similar to the differences between predicted and observed cross sections for heavier atoms. For example, Yeh's values for krypton, one atomic number greater than bromine, predict a 60% greater fall in cross section from He I to He II excitation than that measured by Sampson.[53,54] Another point to note is the intensity behavior of the $^2E_{2g}$ and $^2A_{1g}$ ionizations relative to each other. The ferrocene $^2E_{2g}$-to-$^2A_{1g}$ cross-section ratios are classic examples of the limitations of applying atomic ionization cross sections to molecular ionizations. First, although the $^2E_{2g}$ and $^2A_{1g}$ ionizations are both associated with more than 80% metal 3d character and one would expect a cross-section ratio close to 2:1 on the basis of the orbital degeneracies, the experimental ratio is greater than 4 to 1. This is largely attributed to a molecular effect related to the probabilities for transitions from the vibrational potential well of the neutral molecule to the vibrational levels of the molecular ions. The $^2A_{1g}$ ionization is from a largely nonbonding orbital that results in little geometry change in the positive ion and a sharp ionization, while the $^2E_{2g}$ ionization results in a broader vibrational progression of the positive ion and a larger total cross section. Second, the trend in the $^2E_{2g}$-to-$^2A_{1g}$ cross-section ratios from He I to Ne I excitation does not reflect the slightly different atomic compositions of the orbitals. The ferrocene a_{1g} orbital is more localized on the metal than the e_{2g} orbitals, which are about 10% carbon in character. The carbon 2p cross section increases relative to the iron 3d cross section from He I to Ne I excitation, and the $^2E_{2g}$ ionization peak would be expected to grow in intensity relative to the $^2A_{1g}$ peak. In contrast, the $^2E_{2g}$ ionization diminishes in intensity relative to the $^2A_{1g}$ ionization in the Ne I spectrum. Unusual intensity changes at low photon source energies are typically attributed to "molecular effects" as mentioned in the Introduction, and it is likely that electrons from the a_{1g} orbital are ionized preferentially over the e_{2g} orbital at this photon energy because of a resonance process or some type of autoionization process particular to ferrocene. This intensity behavior has been observed in the Ne I spectrum of unsubstituted ferrocene[70] and every ferrocene derivative studied in our laboratory. The reader is referred to recent work by Stener and Decleva[26] for a detailed density functional theoretical treatment of photoionization cross sections in ferrocene. Regardless of the explanation for this behavior, these results illustrate that atomic ionization cross sections can have limited utility in the interpretation of molecular ionizations, but the relative ionization cross sections of molecular functional groups, once known, can aid interpretation of electronic structure interactions in other molecules.

Figure 11 shows a comparison among cross-section ratios derived from 6-ferrocenylhexanethiol and theoretical cross-section ratios for sulfur 3p and iron 3d atomic orbitals. The theoretical cross-section ratios for the S 3p atomic orbitals compared to Fe 3d atomic orbitals predict a dramatic falloff of sulfur intensity relative to iron with increasing photon energy. While the sulfur lone-pair ionization intensity does indeed follow this prediction, the relative decrease between Ne I and He I is approximately half of that predicted.

Conclusions

The experimental relative photoelectron intensity ratios reported here provide a foundation for an empirical understanding of cross-section behavior in molecules. Gathering ionization intensity ratios for chemical functional groups will assist in explaining intensity changes and interpreting ionizations in the photoelectron spectra of larger and more complex molecules. In general, as the photon energy is varied, the ionization intensity differences observed for molecules are more gradual and show specific deviations from expectations based on calculated atomic cross sections in the low photon energy region (15−45 eV).

Although this may partially be due to assumptions in theoretical calculations of atomic cross sections, molecular effects likely play a large part. The nature of an atomic orbital is significantly different in a molecule, as is the variety of interactions with the ionizing radiation and the description of the outgoing electron in the threshold regime, making molecular spectroscopy distinctly different from atomic spectroscopy. These data provide an experimental foundation for more sophisticated theoretical approaches to calculating molecular ionization cross sections. Regardless of the theoretical explanation for these photoionization cross sections, the empirical intensity ratios reported here and in the future will be of use for developing a familiarity with the low photon energy photoelectron spectra of large molecules containing common functional groups and will aid the assignment and interpretation of complicated photoelectron spectra. The relative ionization intensities of the functional groups studied here show a high degree of transferability between these molecules.

Acknowledgment. We thank the Department of Energy (Division of Chemical Science, Office of Basic Energy Sciences, Office of Energy Research, Grant No. DE-FG03-95ER14574), the National Science Foundation (Grant No. 0078457), and the Materials Characterization Program, Department of Chemistry, the University of Arizona. This article is dedicated with admiration and respect to Professor J. L. Beauchamp on the occasion of his 60th birthday and for his guidance of his former students from whom we also have learned so much.

Supporting Information Available: Figures of all spectra showing spectral fits and tables of the peak areas for these fits along with their assignments. This material is available free of charge via the Internet at http://pubs.acs.org.

References and Notes

(1) Einstein, A. *Ann. Phys.* **1905**, *17*, 549.
(2) Bates, D. R. *Mon. Not. R. Astron. Soc.* **1946**, *106*, 432.
(3) Manson, S. T. *Adv. Electron. Electron Phys.* **1976**, *41*, 73.
(4) Becker, U.; Shirley, D. A. In *VUV and Soft X-ray Photoionization*; Becker, U., Shirley, D. A., Eds.; Plenum: New York, 1996; p 135.
(5) Manson, S. T. In *X-ray and vacuum ultraviolet interaction data bases, calculations, and measurements*; Del Grande, N. K., Lee, P., Samson, J. A. R., Smith, D. Y., Eds.; Proceedings of SPIE—the International Society for Optical Engineering, Vol. 911; SPIE—the International Society for Optical Engineering: Bellingham, WA, 1988; p 2.
(6) Manson, S. T. *Nucl. Instrum. Methods Phys. Res.* **1989**, *A280*, 173.
(7) Federman, S. R.; Lambert, D. L. *J. Electron Spectrosc. Relat. Phenom.* **2002**, *123*, 161−171.
(8) Hatano, Y. *Radiat. Environ. Biophys.* **1999**, *38*, 239.
(9) Green, N. J. B.; Bolton, C. E.; Spencer-Smith, R. D. *Radiat. Environ. Biophys.* **1999**, *38*, 221.
(10) Green, J. C. *Struct. Bonding (Berlin)* **1981**, *43*, 37.
(11) Lichtenberger, D. L.; Kellogg, G. E. *Acc. Chem. Res.* **1987**, *20*, 379.
(12) Green, J. C. *Acc. Chem. Res.* **1994**, *27*, 131.
(13) Lichtenberger, D. L.; Gruhn, N. E.; Renshaw, S. K. *J. Mol. Struct.* **1997**, *405*, 79.
(14) Gruhn, N. E.; Lichtenberger, D. L. In *Inorganic Electronic Structure and Spectroscopy*; Lever, A. B. P., Solomon, E. I., Eds.; John Wiley & Sons: New York, 1999; Vol. II, p 533.
(15) Dechant, P.; Schweig, A.; Thiel, W. *Angew. Chem.* **1973**, *85*, 358.
(16) Guest, M. F.; Hillier, I. H.; Higginson, B. R.; Lloyd, D. R. *Mol. Phys.* **1975**, *29*, 113.
(17) Li, X. R.; Bancroft, G. M.; Puddephatt, R. J. *Acc. Chem. Res.* **1997**, *30*, 213.
(18) Langhoff, P. W.; Padial, N.; Csanak, G.; Rescigno, T. N.; McKoy, B. V. *Int. J. Quantum Chem.* **1980**, *14*, 285−304.
(19) Cacelli, I.; Carravetta, V.; Rizzo, A.; Moccia, R. *Phys. Rep.* **1991**, *205*, 283.
(20) Amusia, M. Y. In *VUV and Soft X-ray Photoionization*; Becker, U., Shirley, D. A., Eds.; Plenum: New York, 1996; p 1.
(21) Rescigno, T. N.; Orel, A. E.; McCurdy, C. W. *Phys. Rev. A* **1997**, *55*, 342−346.
(22) Stener, M.; Decleva, P. *J. Chem. Phys.* **2000**, *112*, 10871.
(23) Stener, M.; Fronzoni, G.; Furlan, S.; Decleva, P. *J. Chem. Phys.* **2001**, *114*, 306 and references therein.
(24) Cacelli, I.; Moccia, R.; Montuoro, R. *Chem Phys. Lett.* **2001**, *347*, 261−267.
(25) Potts, A. W.; Trofimov, A. B.; Schirmer, J.; Holland, D. M. P.; Karlsson, L. *Chem. Phys.* **2001**, *271*, 337−356.
(26) Fronzoni, G.; Colavita, P.; Stener, M.; De Alti, G.; Decleva, P. *J. Phys. Chem. A* **2001**, *105*, 9800.
(27) Dupin, H.; Baraille, I.; Larrieu, C.; Relat, M.; Dargelos, A. *J. Mol. Struct. (THEOCHEM)* **2002**, *577*, 17.
(28) Toffoli, D.; Stener, M.; Fronzoni, G.; Decleva, P. *Chem. Phys.* **2002**, *276*, 25−43.
(29) Lin, P.; Lucchese, R. R. *J. Chem. Phys.* **2002**, *116*, 8863−8875.
(30) Cooper, G.; Green, J. C.; Payne, M. P.; Dobson, B. R.; Hillier, I. H. *Chem. Phys. Lett.* **1986**, *125*, 97.
(31) Cooper, G.; Green, J. C.; Payne, M. P.; Dobson, B. R.; Hiller, I. H. *J. Am. Chem. Soc.* **1987**, *109*, 3836.
(32) Trofimov, A. B.; Koppel, H.; Schirmer, J. *J. Chem. Phys.* **1998**, *109*, 1025 and references therein.
(33) Brennan, J. G.; Green, J. C.; Redfern, C. M. *J. Am. Chem. Soc.* **1989**, *111*, 2373.
(34) The Ne I spectrum of oxygen is a dramatic example of autoionization effects at low photon energies. See: Price, W. C. In *Electron Spectoscopy: Theory, Techniques and Applications*; Brundle, C. R., Baker, A. D., Eds.; Academic Press: New York, 1977; Vol. 1, p 152.
(35) Cooper, J.; Zare, R. N. *J. Chem. Phys.* **1968**, *48*, 942.
(36) Manson, S. T. *J. Electron. Spectrosc. Relat. Phenom.* **1993**, *66*, 117.
(37) Chidsey, C. E. D.; Bertozzi, C. R.; Putviinski, T. M.; Mujsce, A. M. *J. Am. Chem. Soc.* **1990**, *112*, 4301.
(38) Lichtenberger, D. L.; Kellogg, G.; Kristofzski, J. G.; Page, D.; Turner, S.; Klinger, G.; Lorenzen, J. *Rev. Sci. Instrum.* **1986**, *57*, 2366.
(39) Westcott, B. L.; Gruhn, N. E.; Enemark, J. H. *J. Am. Chem. Soc.* **1998**, *120*, 3382 and references therein.
(40) Lichtenberger, D. L.; Fenske, R. F. *J. Am. Chem. Soc.* **1976**, *98*, 50.
(41) Lichtenberger, D. L.; Copenhaver, A. S. *J. Electron Spectrosc. Relat. Phenom.* **1990**, *50*, 335.
(42) Bevington, P. R. *Data Reduction and Error Analysis for the Physical Sciences*; McGraw-Hill: New York, 1969.
(43) Copenhaver, A. S. *Diss. Abstr. Int. B* **1989**, *50*, 3464.
(44) Baerends, E. J.; Ellis, D. E.; Ros, P. *Chem. Phys.* **1973**, *2*, 41.
(45) te Velde, G.; Baerends, E. J. *J. Comput. Phys.* **1992**, *99*, 84.
(46) Bickelhaupt, F. M.; van Eikema Hommes, N. J. R.; Guerra, C. F.; Baerends, E. J. *Organometallics* **1996**, *15*, 2923.
(47) Guerra, C. F.; Snijders, J. G.; te Velde, G.; Baerends, E. J. *Theor. Chem. Acc.* **1998**, *99*, 391.
(48) Becke, A. D. *Phys. Rev. A* **1988**, *38*, 3098.
(49) Lee, C.; Yang, W.; Parr, P. G. *Phys. Rev. B* **1988**, *37*, 785.
(50) Frisch, M. J.; Trucks, G. W.; Schlegel, H. B.; Scuseria, G. E.; Robb, M. A.; Cheeseman, J. R.; Zakrzewski, V. G.; Montgomery, J. A., Jr.; Stratmann, R. E.; Burant, J. C.; Dapprich, S.; Millam, J. M.; Daniels, A. D.; Kudin, K. N.; Strain, M. C.; Farkas, O.; Tomasi, J.; Barone, V.; Cossi, M.; Cammi, R.; Mennucci, B.; Pomelli, C.; Adamo, C.; Clifford, S.; Ochterski, J.; Petersson, G. A.; Ayala, P. Y.; Cui, Q.; Morokuma, K.; Malick, D. K.; Rabuck, A. D.; Raghavachari, K.; Foresman, J. B.; Cioslowski, J.; Ortiz, J. V.; Stefanov, B. B.; Liu, G.; Liashenko, A.; Piskorz, P.; Komaromi, I.; Gomperts, R.; Martin, R. L.; Fox, D. J.; Keith, T.; Al-Laham, M. A.; Peng, C. Y.; Nanayakkara, A.; Gonzalez, C.; Challacombe, M.; Gill, P. M. W.; Johnson, B. G.; Chen, W.; Wong, M. W.; Andres, J. L.; Head-Gordon, M.; Replogle, E. S.; Pople, J. A. *Gaussian 98*, revision A.7; Gaussian, Inc.: Pittsburgh, PA, 1998.
(51) *SPARTAN SGI*, version 5.1.3; Wavefunction Inc.: 18401 Von Karman Ave. #370, Irvine, CA 92612.
(52) Cooper, G.; Burton, G. R.; Brion, C. E. *J. Electron Spectrosc. Relat. Phenom.* **1995**, *73*, 139.
(53) Samson, J. A. R.; Yin, L. *J. Opt. Soc. Am. B* **1989**, *6*, 2326−2333.
(54) Samson, J. A. R.; Stolte, W. C. *J. Electron Spectrosc. Relat. Phenom.* **2002**, *123*, 265−276.
(55) Yeh, J. J.; Lindau, I. *At. Data Nucl. Data Tables* **1985**, *32*, 1.
(56) Yeh, J. J. *Atomic Calculation of Photoionization Cross Sections and Asymmetry Parameters*; Gordon and Breach Science Publishers: Langhorne, PA, 1993.
(57) Verner, D. A.; Yakovlev, D. G.; Band, I. M.; Trzhaskovskaya, M. B. *At. Data Nucl. Data Tables* **1993**, *55*, 233−280.
(58) Trzhaskovskaya, M. B.; Nefedov, V. I.; Yarzhemsky, V. G. *At. Data Nucl. Data Tables* **2001**, *77*, 97.
(59) Novak, I.; Ng, S. C.; Jin, S.; Huang, H. H.; Huang, W. *J. Phys. Chem. A* **1997**, *101*, 3501−3504.
(60) Potts, A. W.; Edvardsson, D.; Karlsson, L.; Holland, D. M. P.; MacDonald, M. A.; Hayes, M. A.; Maripuu, R.; Siegbahn, K.; von Niessen, W. *Chem. Phys.* **2000**, *254*, 385−405.

(61) Casarin, M.; Pandolfo, L.; Vittadini, A. *Organometallics* **2001**, *20*, 754−762.
(62) Novak, I.; Li, D. B.; Kovač, B. *J. Phys. Chem. A* **2002**, *106*, 2850−2854.
(63) Novak, I.; Li, D. B.; Potts, A. W. *J. Phys. Chem. A* **2002**, *106*, 465−468.
(64) Gelius, U.; Siegbahn, K. *Faraday Discuss. Chem. Soc*. **1972**, 257.
(65) Yang, C. N. *Phys. Rev*. **1948**, *74*, 764.
(66) Ashby, M. T.; Enemark, J. H.; Lichtenberger, D. L. *Inorg. Chem.* **1988**, *27*, 191.
(67) Evans, S.; Green, M. L. H.; Jewitt, B.; Orchard, A. F.; Pygall, C. F. *J. Chem. Soc., Faraday Trans. 2* **1972**, *68*, 1847.
(68) Cauletti, C.; Green, J. C.; Kelly, M. R. *J. Electron. Spectrosc. Relat. Phenom.* **1980**, *19*, 327 and references therein.
(69) Cooper, G.; Green, J. C.; Payne, M. P. *Mol. Phys.* **1988**, *63*, 1031.
(70) Westcott, B. L. *Diss. Abstr. Int. B* **1997**, *58*, 4218.